11A.2   A MULTI-DOPPLER ANALYSIS OF CONVECTIVE INITIATION ON 10 JUNE 2002 DURING IHOP_2002

Nettie R. Arnott*
Yvette P. Richardson
The Pennsylvania State University, University Park, Pennsylvania

Joshua M. Wurman
Center for Severe Weather Research, Boulder, Colorado

1.   INTRODUCTION

Forecasts of the initiation of deep moist convection are important in a variety of meteorological applications: flash flood, severe storm, and quantitative precipitation forecasting. Determining where and when convection occurs affects the aircraft and agriculture industries as well as the general public.

Recently, the research community has placed a strong emphasis on factors that determine the likelihood of convection initiation. Field experiments have increased understanding of the processes leading to initiation. For example, Atkins et al. (1995) and Weckwerth (2000) observed horizontal convective rolls (HCRs) along a sea-breeze in Florida and found that their kinematic and thermodynamic properties played a significant roll in convection initiation. Similarly, Fankhauser et al. (1995) found that merging of thunderstorm gust fronts with HCRs lead to initiation. Other favored locations include discontinuities or kinks along a front (Kingsmill, 1995). Often, small variations in surface moisture and temperature have a profound effect on whether thunderstorms form (Mueller et al. 1993).

Numerical simulations have also advanced understanding of convection initiation. For example, Crook (1996) used numerical simulations to conclude that variations in boundary layer temperature and moisture as small as 1 C and 1 gm kg^{-1} respectively can distinguish between no convection and intense convection. Lee et al. (1991) demonstrated how small variations in vertical shear, moisture, and convergence along a boundary can greatly affect the likelihood and timing of initiation, and the storm intensity when initiation occurs.

Each of these studies suggests that observations of small scale variations in the thermodynamic and kinematic fields are necessary for understanding the processes that initiate convection. To this end, the International H_2O Project (IHOP) gathered many ground-based and airborne research platforms in order to observe the effects of small-scale water vapor inhomogeneities in initiating convection. While airborne platforms surveyed a large region, ground-based assets were focused mainly within an intensive observation region (IOR) defined by the locations of the mobile Doppler radars. The IOR of each deployment was confined to approximately a 20 km by 20 km quadrilateral, obtaining high resolution observations to determine the role of water vapor in initiating convection.

In accord with the goals of IHOP, this particular study attempts to characterize the properties of the wind and water vapor fields on 10 June 2002, and examine the interaction of these fields and their influence on storm initiation. Multi-Doppler wind syntheses are here examined to determine the kinematic structure of the boundary layer, and ultimately will be linked with airborne lidar measurements and surface in-situ data to examine the water vapor field.

On 10 June 2002, the Doppler on Wheels (DOW) mobile radars, the XPOL radar, and the Shared Mobile Atmospheric Research and Teaching radar (SMART-R) along with the rest of the IHOP armada continuously observed a quasi-stationary cold front for three hours. The boundary layer structure transitions from horizontal convective rolls (HCRs) behind the cold front to open cell convection ahead of the front. As observed by Atkins et al. (1998) and Wilson et al. (1992), misocyclones are located along the cold front prior to initiation. The multi-Doppler analyses provide the kinematic structure and evolution of these circulations. The corresponding water vapor field will be examined to determine the relationship of these circulations to the moisture variability along the front. Additionally, the evolution of the cold frontal depth and moisture convergence will be studied to determine why a lull in cloud growth occurred in the hour before convection initiated on the edge of the IOR and why convection did not initiate along the intensely observed portion of the front.

2.   METHOD

2.1 Data Collection

On 10 June 2002, the mobile radars formed the corners of an IOR north of Ness City, Kansas (Fig. 1a). Data were collected from 1900 UTC to 22:30 UTC. Within the IOR, overdetermined multi-Doppler analyses are possible. The unambiguous range of the radars allow for data collection outside of the IOR, hence dual- and tri-Doppler analyses can also be examined in surrounding regions.

2.2 Data Analysis

Corresponding author address: Nettie Arnott
Dept. of Meteorology, The Pennsylvania State University, University Park, PA 16802; email:
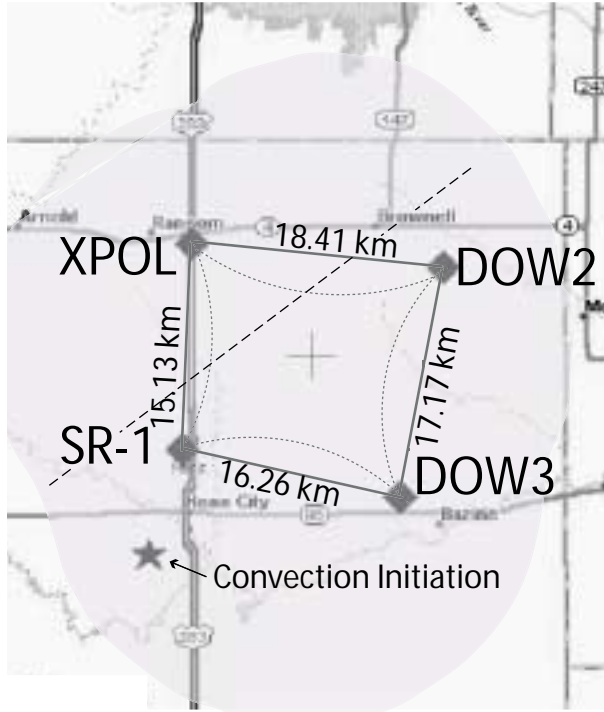narnott@met.psu.edu

Fig. 1 (a). Locations of mobile radars (diamonds) on 10 June 2002. Solid lines form the sides of the IOR with lengths as shown. Long dashed line is the approximate cold front location. Within the region bounded by the short dashed curves, quadruple -Doppler analyses are possible. The shaded region denotes the area in which dual-Doppler data are available.

We undertake a semi-automated approach using NCAR's SOLO program to remove ground clutter from the radar data. Because ground clutter targets such as towers and trees can influence the velocity field beyond the specific target location, fairly low reflectivity criteria are established to remove the "low-velocity rings" of and around the ground clutter.

The Bargen-Brown scheme (Bargen and Brown, 1980) is used for the majority of the unfolding. Manual dealiasing is required in regions where the automated scheme fails.

Before the radar data can be synthesized to a common earth-relative grid, several corrections are applied. First, the data azimuths must be made earth-relative by adding an offset based on the truck orientation. This offset is found using a solar alignment technique (Arnott et al. 2003).

We also apply a correction for the azimuth assigned to each ray. The DOW radars prescribe the azimuth of each ray when the antenna is at the end of the integration period rather than the center. The following correction is applied to the azimuth of each ray

$$\phi_{new} = \phi_{old} - \frac{\partial \phi}{\partial t} \Delta t \qquad (1)$$

where (ϕ_{new}) is the corrected azimuth, the rotation rate is given by

$$\frac{\partial \phi}{\partial t} = \frac{\phi_1 - \phi_0}{t_1 - t_0}, \qquad (2)$$

and Δt is the interpulse period time the number of pulses used in the integration. The magnitude of this correction is approximately .3 degrees for each ray.

Preliminary Barnes objective analyses are produced using REORDER with smoothing parameters chosen to eliminate scales near those of the data spacing and a cut-off radius equal to approximately 2.5 times the coarsest data spacing in the grid. CEDRIC is used to produce the dual-Doppler synthesis, using upward integration.

3. SYNOPTIC ENVIRONMENT

The surface analysis for 10 June 2002 at 2100 UTC shows the quasi-stationary cold front observed by the radars (Fig. 2). Convection initiates 10 minutes later. Strong southerly winds off the Gulf of Mexico help provide low level moisture over the IOR. Post-frontal air is significantly drier. Convection first initiates to the south near the intersection of the cold front with the dryline. Storms subsequently initiate north east along the cold front.

A 5580 decameter low at 500 mb (not shown) is centered over Idaho. A weak diffluent region exists over the IOR at 12 UTC on the morning of 10 June 2002. At 850 mb (not shown), the low is centered over North Dakota. This places the IOR beneath a dry continental southwest flow.

The 1200 UTC Dodge City, KS sounding also shows dry air at midlevels (Fig.3). Instability is significant with 2600 J/kg of CAPE. Southerly winds at the surface and westerly winds aloft produce strong directional shear.

4. RESULTS

High resolution data were collected on the quasi-stationary cold front by all four mobile radars. Observed features include small scale circulations (misocylcones) along the boundary and HCRs perpendicular to the boundary. Preliminary dual-Doppler analyses during the 30 minutes before convection initiation from DOW2 and DOW3 are shown in Fig. 4. The location of the boundary is evident by the horizontal wind shift and enhanced vertical velocity. At the time of initiation, the 2 dbZ contour (Fig.4 d) clearly depicts the boundary and the storm slightly ahead of it. Typical vertical velocities along the front are 1 ms^{-1}.

The locations of vorticity maxima along the boundary coincide with vertical velocity maxima in some instances, while in other cases they lie in regions of weak upward motion. Cross sections through the misocyclones at 2110UTC near (0,0) and (2,3) are shown in Figs. 5a and 5b, respectively. The circulations extend from the surface to about 1.6 km and coincide with reflectivity maxima along the boundary (not shown). In the circulation near (0,0), a ring of upward velocities surrounds the circulation, while subsidence blankets the misocyclone near (2,3). Nevertheless rising air is present just north and south of this circulation (not shown). These preliminary results are unlike those found in previous studies and a
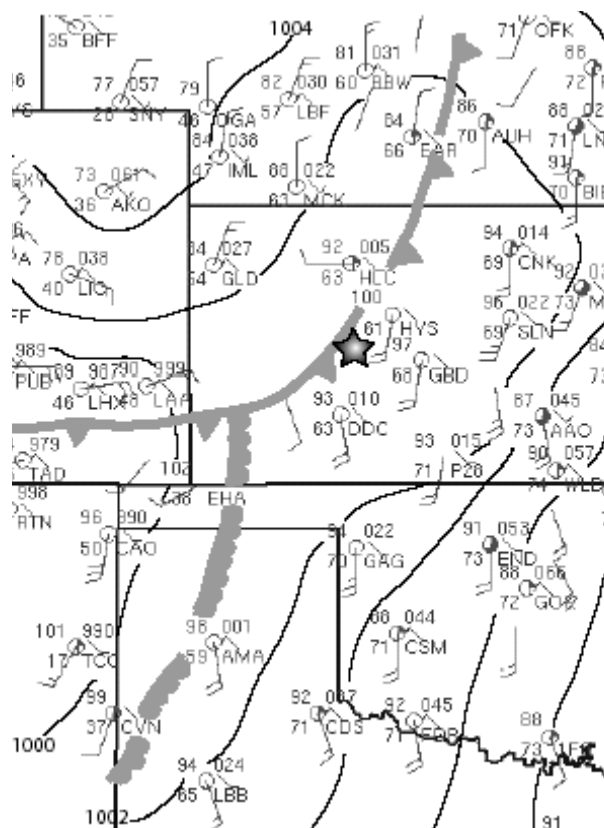
Fig. 2. Surface analysis for 10 June 2002 at 2100 UTC (10 minutes before convection initiation). Sea-level pressure is contoured at 2-mb intervals. Surface cold front, dryline, and station plots have conventional symbols. The star represents the location of the IOR.

Fig. 3. 10 June 2002 1200 UTC Dodge City, KS sounding. Winds are in knots with a full barb equaling 10 knots.

concurrent study by Richardson et al. (2003). In these studies the misocycloness are consistently displaced to the south of vertical velocity maxima. The relationship between misocyclone location and vertical velocity on 10 June 2002 will be examined in more detail.

The HCRs and open cell convection occur earlier in the deployment and are presently not distinguishable at the times shown.

5. FUTURE WORK

Additional study will include sensitivity tests of the objective analysis to factors such as the smoothing parameter and cut off radius. We also will examine sensitivities of the dual-Doppler syntheses to different integration methods.

Multi-Doppler analyses will include XPOL and SMART-R data. Furthermore, water vapor observations will be combined with the multi-Doppler analyses in order to understand the effects of the misocyclones, HCRs, open cell convection, and boundary on the moisture distribution. Superposition of parcel trajectories and cloud locations on these analyses will help isolate the features effective at lifting parcels to their level of free convection.

While convection initiation is observed in the dual-Doppler domain, the boundary layer forcing mechanisms may lie too far from the center of the IOR to determine the 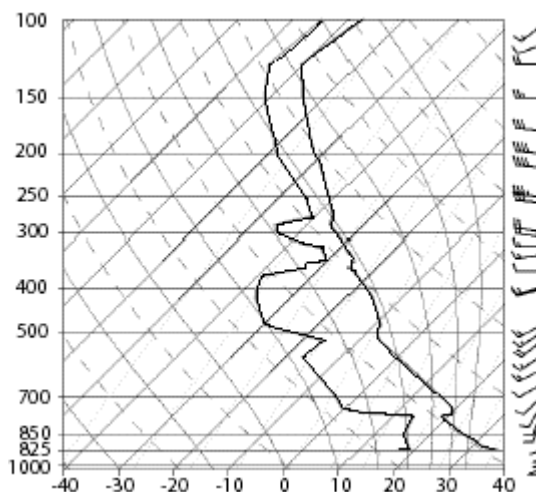causes of initiation. Nevertheless, high-resolution data within the IOR are available for determining why initiation did not occur along this portion of the boundary.

REFERENCES

Arnott, N. R., Y. P. Richardson, J. M. Wurman, and J. Lutz, 2003: A solar alignment technique for determining mobile radar pointing angles. Preprints, *31st Conference on Radar Meteorology,* 6-12 August, 2003, Seattle, WA., Amer. Meteor. Soc., this issue.

Atkins, N. T., R. M. Wakimoto, and T. M. Weckwerth 1995: Observations of the sea-breeze front during CaPE. Part II: Dual-Doppler and aircraft analysis. *Mon. Wea. Rev.*, **123**, 994 - 969.

Crook, N. A., 1996: Sensitivity of moist convection forced by boundary layer processes to low-level thermodynamic fields. *Mon. Wea. Rev.,* **124**, 1767-1785.

Fankhauser, J.C., N.A. Crook, J. Tuttle, L.J. Miller, and C.G. Wade, 1995: Initiation of deep convection along boundary layer convergence lines in a semitropical environment. *Mon. Wea. Rev.,* **123,** 291-313.

Kingsmill, D.E., 1995: Convection initiation associated wit ha sea-breeze front, a gust front, and their collision. *Mon. Wea. Rev.*, **123**, 2913-2932.

Lee, B.D., R. D. Farley, and M.R. Hjelmfelt, 1991: A numerical case study of convection initiation along colliding convergence boundaries in northeast Colorado. J. *Atmos. Science*, **48,** 2350-2365.

Mueller, C.K., J. W. Wilson, and N. A. Crook, 1993: The utility of sounding and mesonet data to nowcast thunderstorm initiation. *Wea. Forecasting*, **8**, 132-146.

Richardson, Y. P., J. M. Wurman, and C. Hartman, 2003: Multi-Doppler analysis of convection initiation on 19 June 2002. Preprints, *31st Conference on Radar Meteorology,* 6-12 August, 2003, Seattle, WA., Amer. Meteor. Soc., this issue.

Weckwerth, T. M., 2000: The effect of small-scale moisture variability on thunderstorm initiation. *Mon. Wea. Rev.*, **128**, 4017-4030.

Wilson, J.W., G. B. Foote, N. Andrew Crook, J. C. Fankhauser, C.G. Wade, J. D. Tuttle, and Cynthia K. Mueller, 1992: The role of boundary-layer convergence zones and horizontal roles in the initiation of thunderstorms: A case study. *Mon. Wea. Rev.*, **120**, 1785-1814.
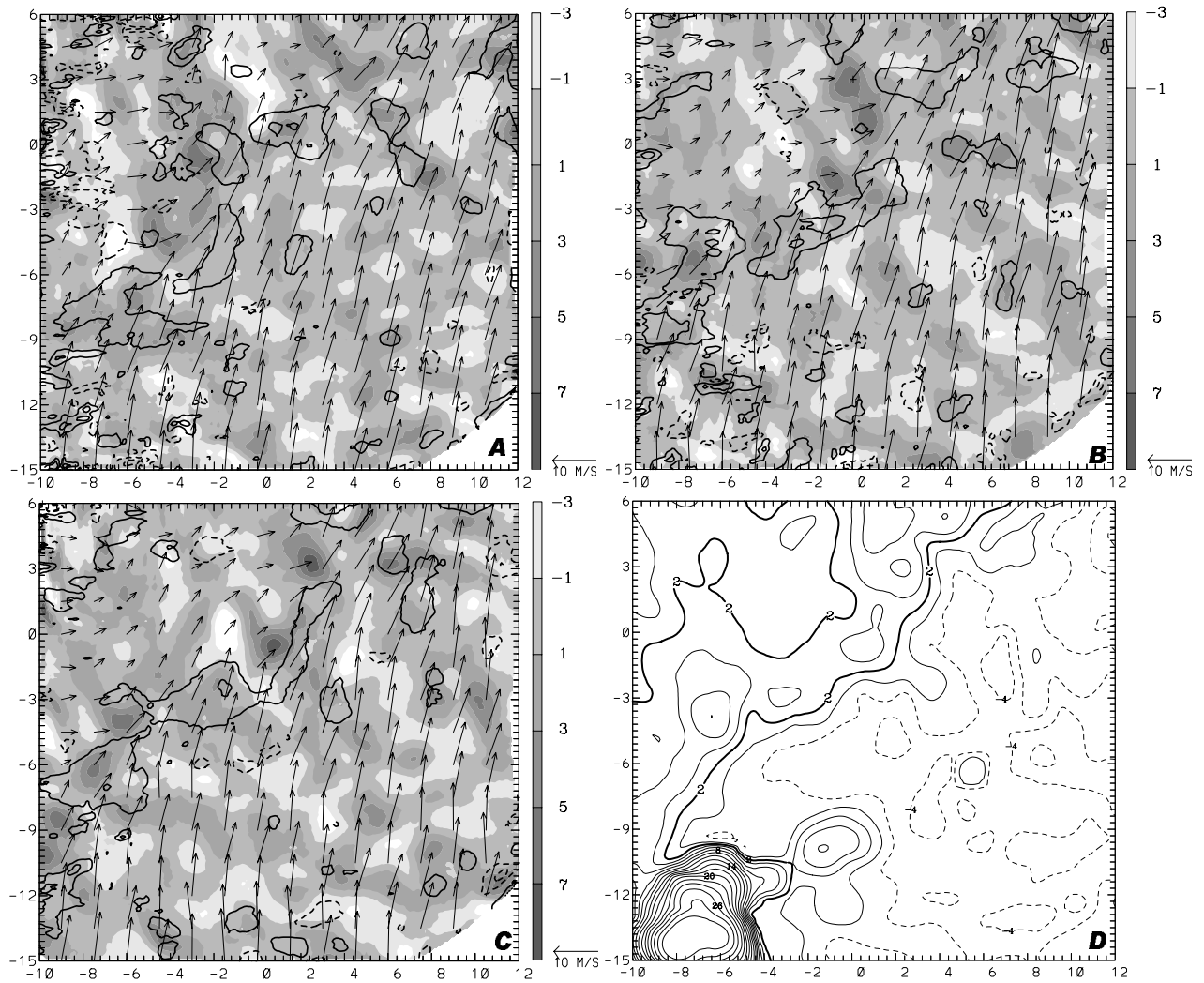
Fig. 4. Dual-Doppler syntheses from DOW2 and DOW3 at z=600 m. Axes are west-east and north-south distance from the grid center in km. DOW2 is at (16km,7 km) and DOW3 is at (13 km,10 km). Vertical vorticity (shaded, scaled by 1000), vertical velocity (contoured every 1 ms^{-1} starting at 1 ms^{-1}, zero contour not shown), horizontal wind (vectors) for (a) 2048 UTC (b) 2103 UTC (c) 2110 UTC. Reflectivity observed by DOW2 at 2110 UTC is shown in (d). The cold front is evident in the shift of horizontal winds, and enhanced vertical velocity and reflectivity. Vorticity maxima represent the locations of misocyclones along the cold front.
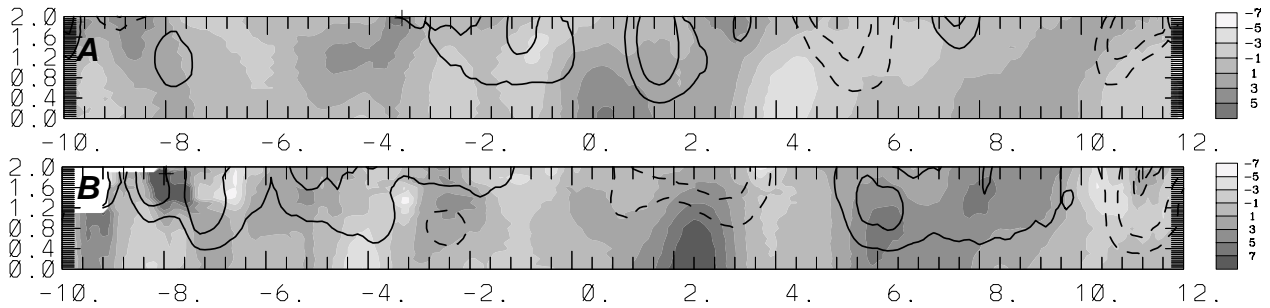

Fig. 5. West-east cross section through (a) y=-1.2 km (b) y=3.4 km. Abscissa is west-east distance in km, ordinate is height in km, Vertical vorticity is shaded (scaled by 1000) and vertical velocity is contoured every 1 ms^{-1} (zero contour not shown), Note the upward motion surrounding the misocyclone at x = 0 km in (a) and the subsidence over the misocyclone at x = 2 km in (b). North-south cross-sections show a pattern similar to that in (a) for both circulations.